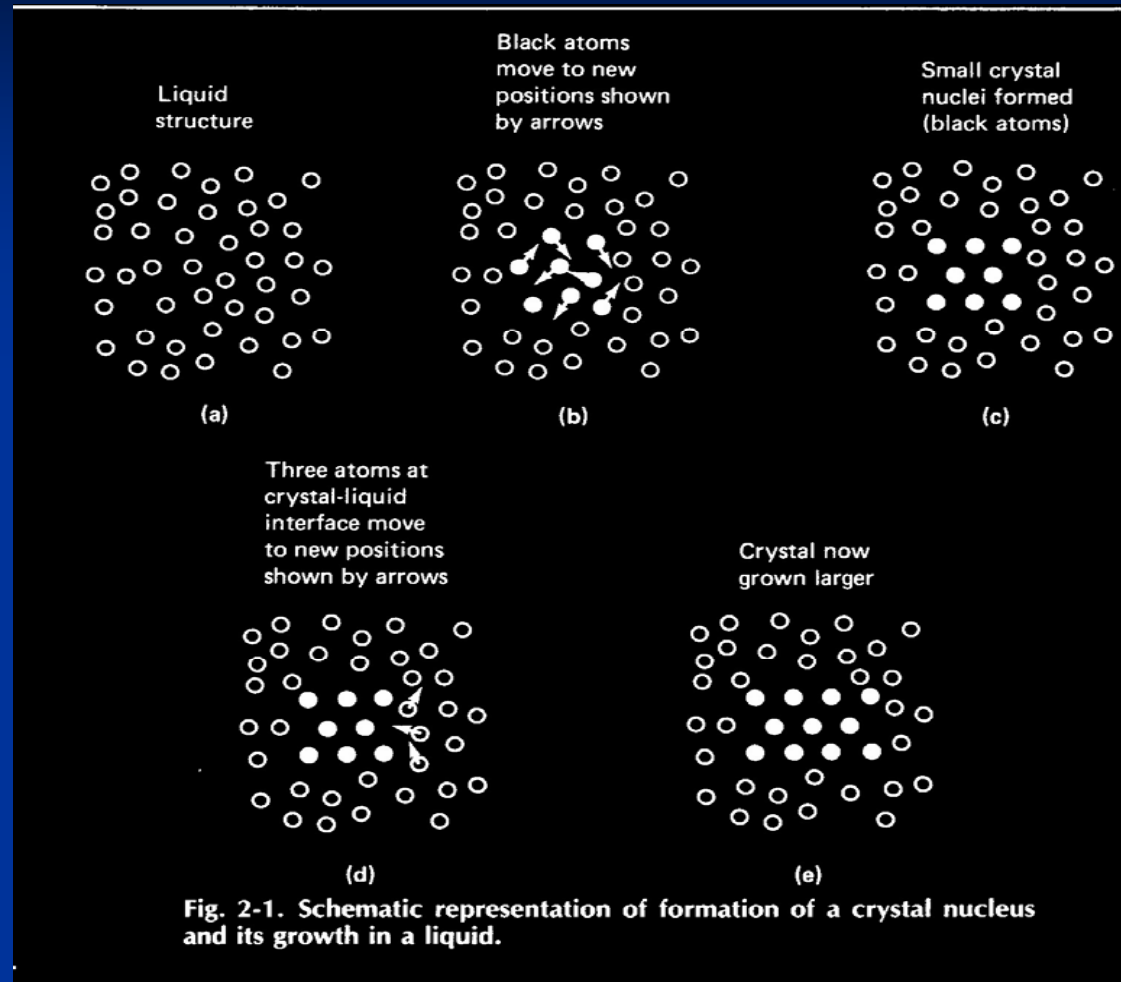
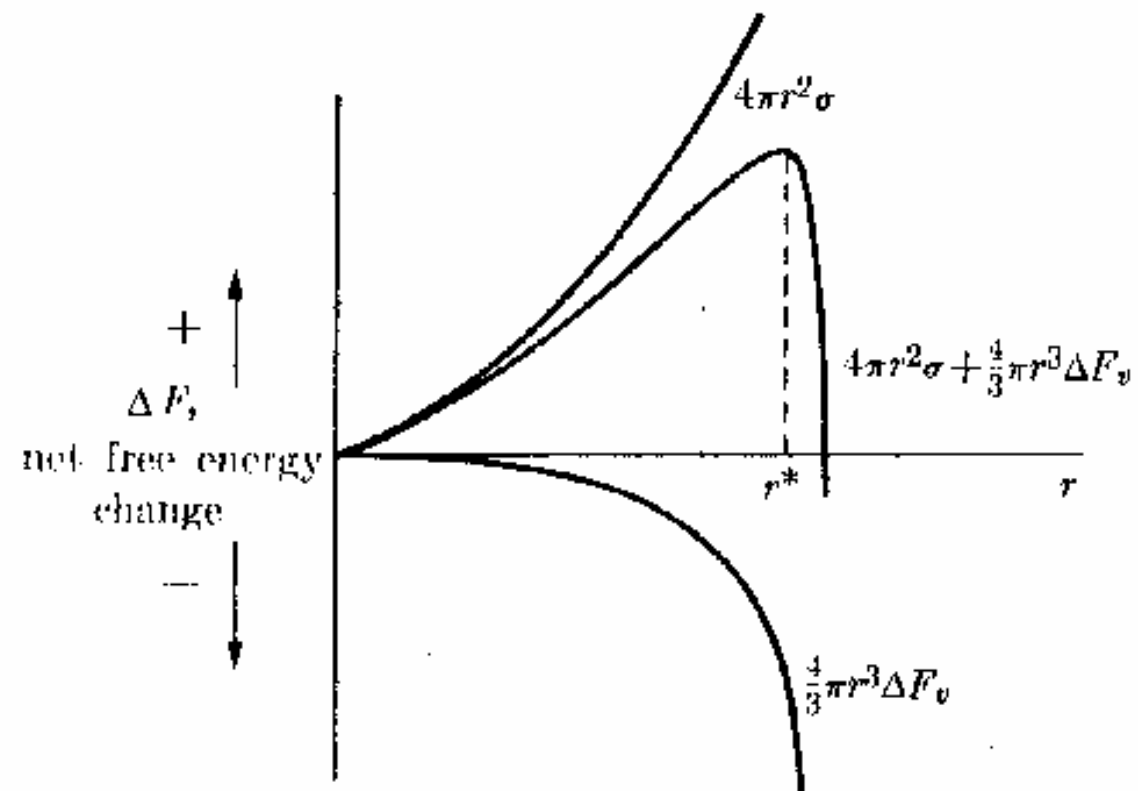


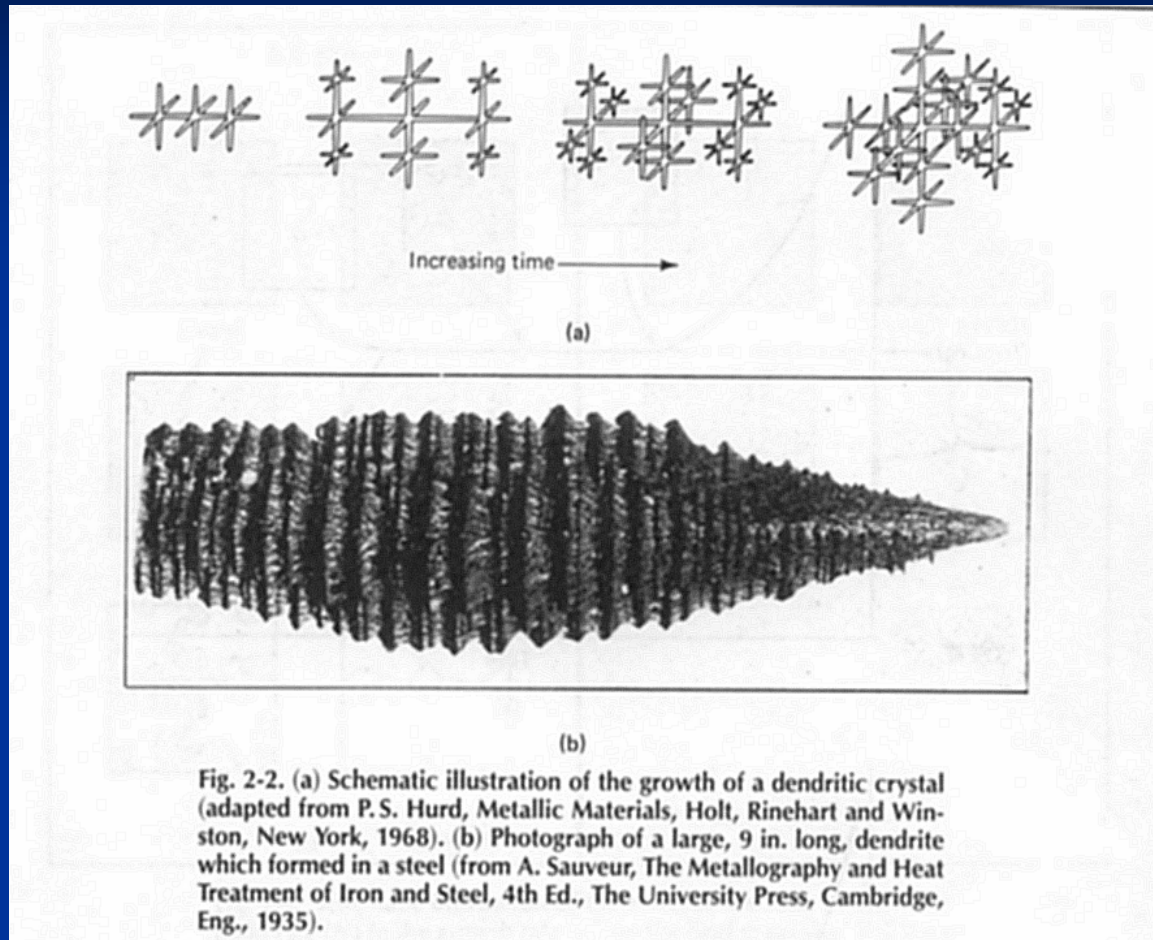
SOLIDIFICACION DE METALES



FORMACION DE NUCLEOS CRISTALINOS EN EL LIQUIDO

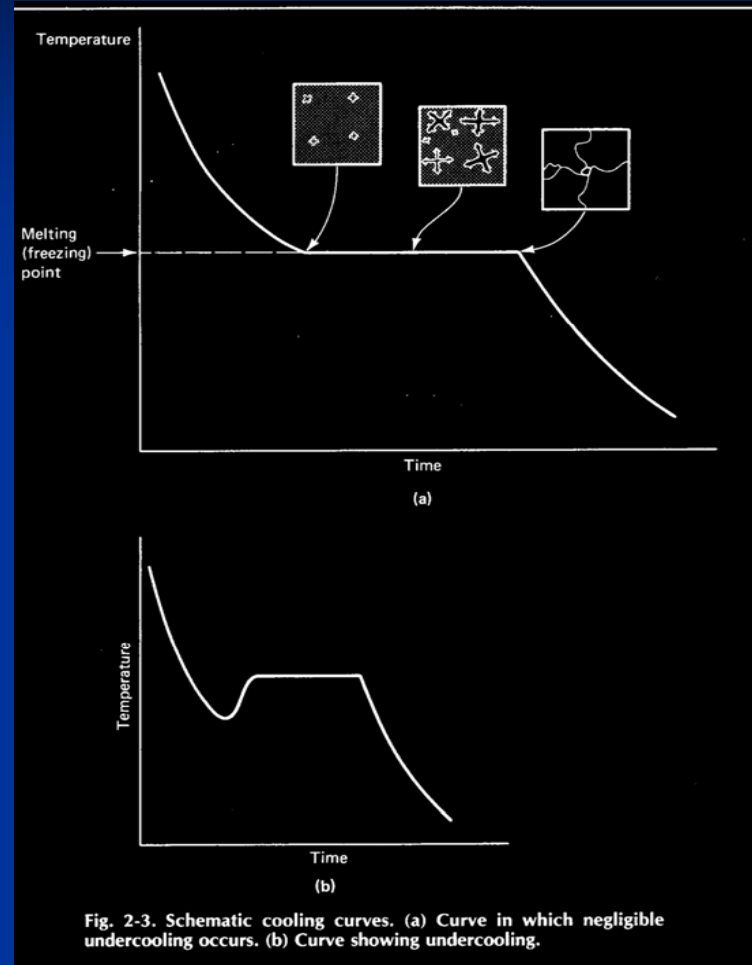


SOLIDIFICACION DE METALES



CRECIMIENTO DENDRÍTICO EN METALES

SOLIDIFICACION DE METALES



CURVAS DE ENFRIAMIENTO METAL PURO

SOLIDIFICACION DE METALES

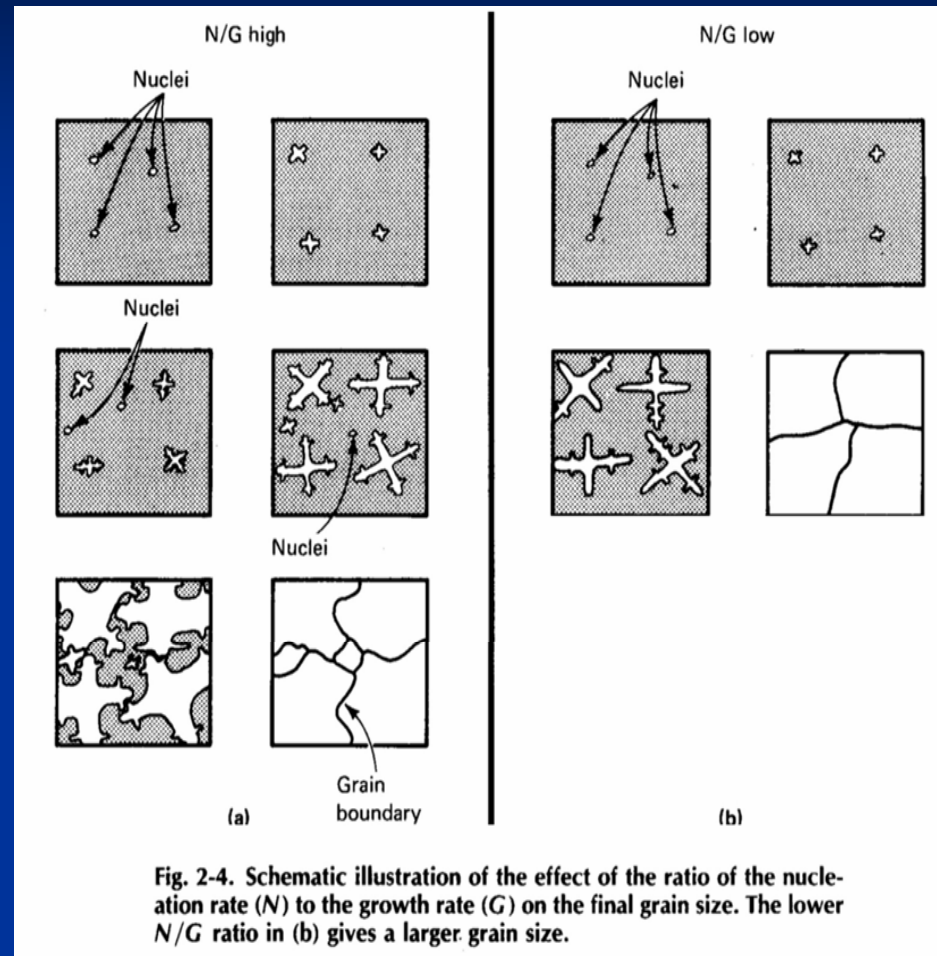


Fig. 2-4. Schematic illustration of the effect of the ratio of the nucleation rate (N) to the growth rate (G) on the final grain size. The lower N/G ratio in (b) gives a larger grain size.

EFFECTO DE LA RAZÓN DE NUCLEACION Y VELOCIDAD DE CRECIMIENTO SOBRE EL TAMAÑO DE GRANO

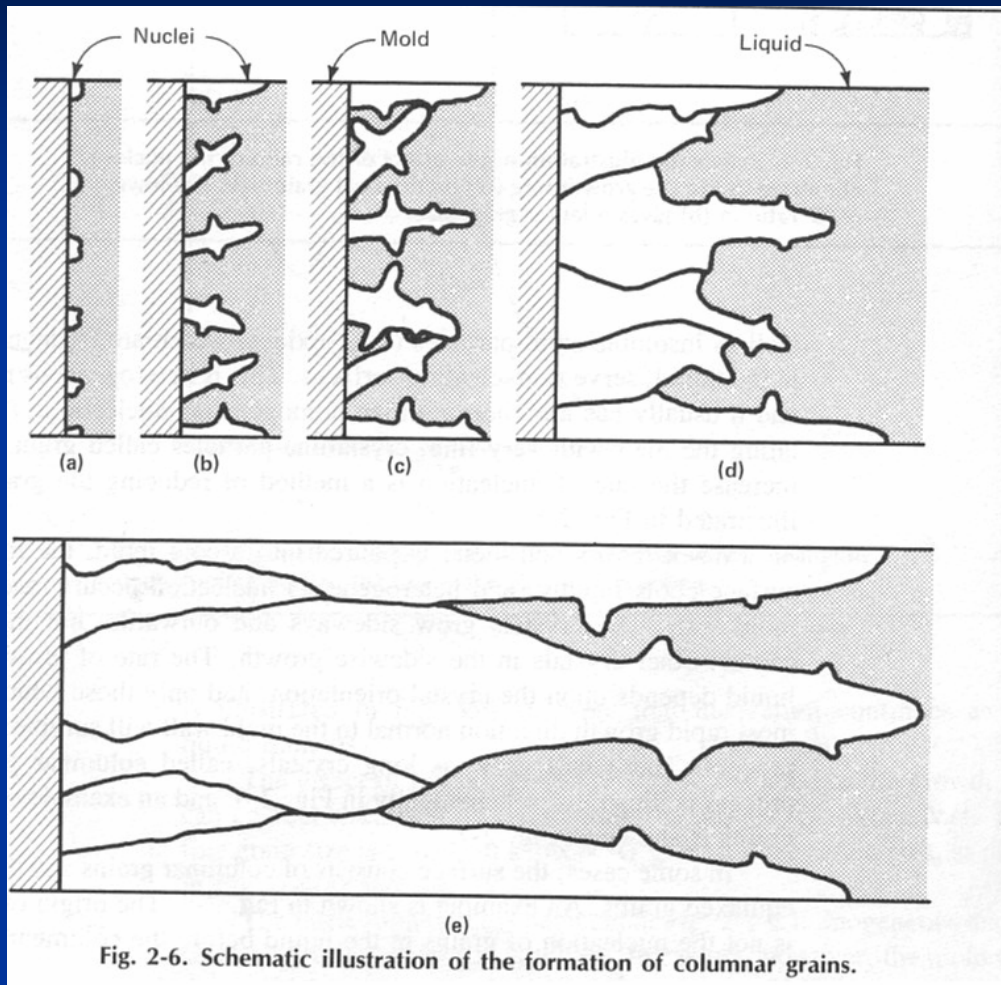
SOLIDIFICACION DE METALES



Fig. 2-5. Effect of addition of a grain refiner on the cast grain size and shape of commercially pure aluminum (1100 aluminum) cast by a two-belt method. Both pictures are of longitudinal sections, shown at actual size. The upper slab was cast without a grain refiner and the lower with a grain refiner addition (e.g., titanium or titanium and boron). (From Metals Handbook, 8th Ed., Vol 8, American Society for Metals, Metals Park, Ohio, 1973)

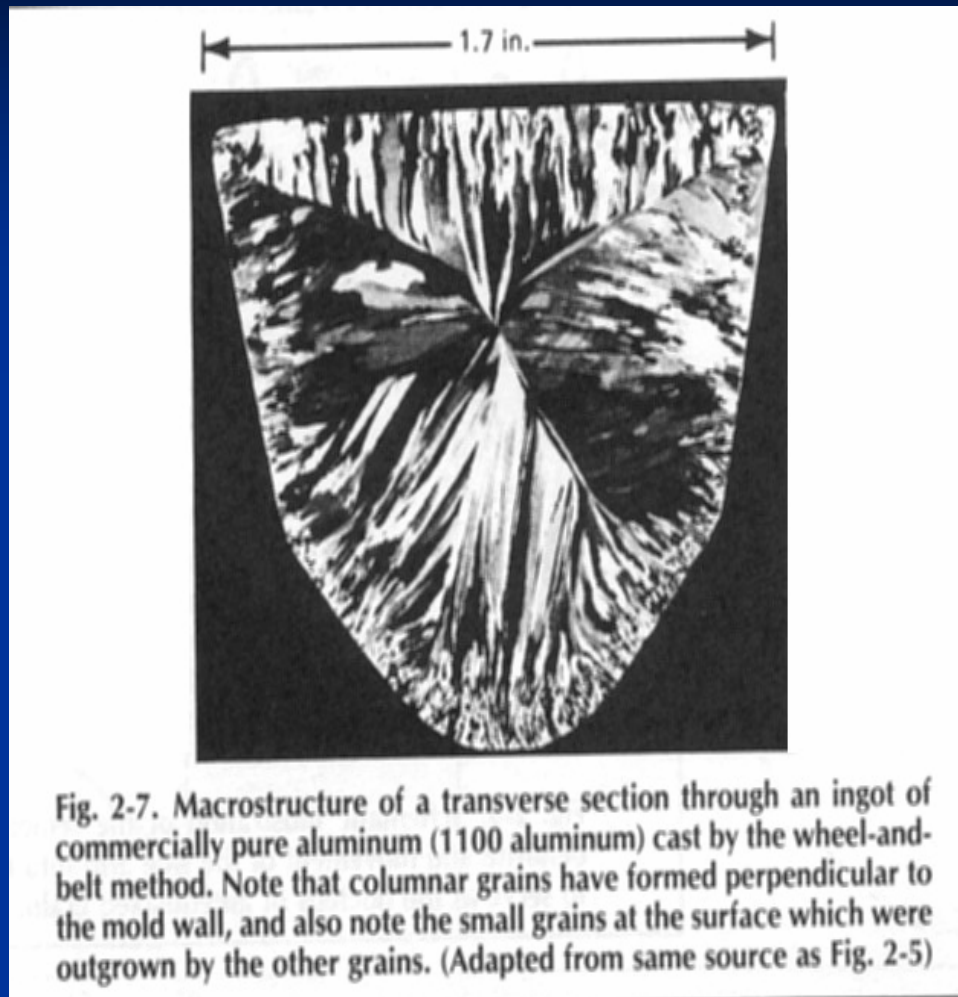
EFFECTO DE AFINANTES SOBRE EL TAMAÑO DE GRANO EN ALUMINIO 1100

SOLIDIFICACION DE METALES



CRECIMIENTO DE GRANOS COLUMNARES

SOLIDIFICACION DE METALES



ESTRUCTURA COLUMNAR EN ALUMINIO 1100

SOLIDIFICACION DE METALES

MACROESTRUCTURA DE SOLIDIFICACION DE UN LINGOTE DE LATÓN DE CORTE LIBRE (360) MOSTRANDO GRANOS COLUMNARES CRECIENDO DESDE LA SUPERFICIE Y GRANOS EQUIAXIALES EN EL CENTRO. LA FOTO SUPERIOR ES UNA SECCION TRANSVERSAL Y LA INFERIOR CORRESPONDE AL FONDO

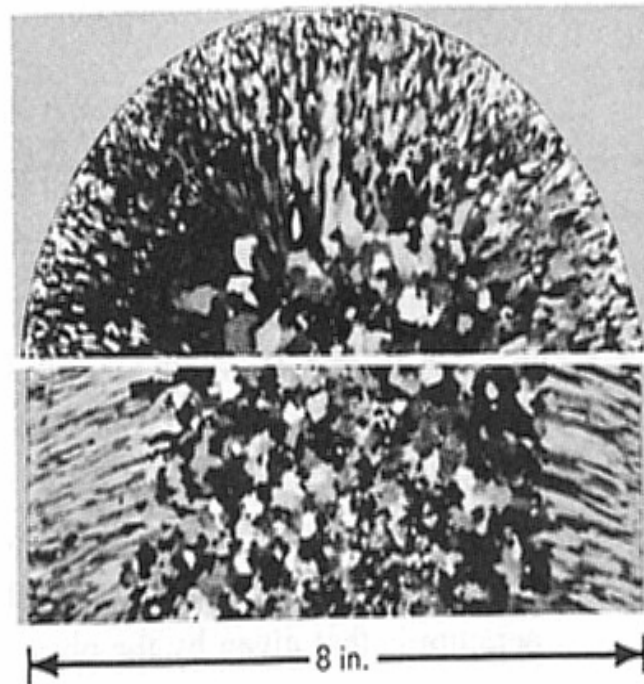
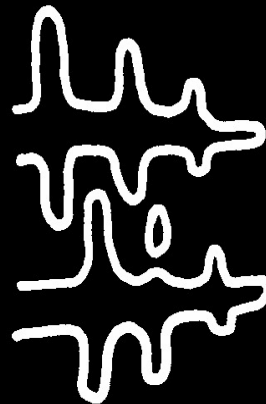
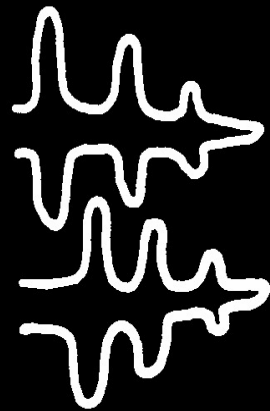
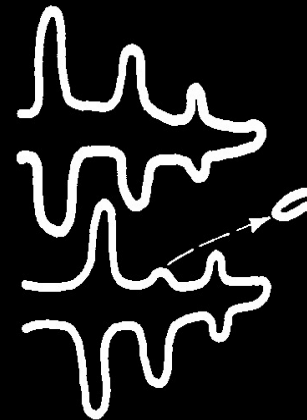


Fig. 2-8. Macrostructure of a static cast ingot of a free-cutting brass (alloy 360), showing columnar grains growing in from the surface and equiaxed grains in the center. The top picture is a transverse section, the bottom longitudinal. (Adapted from same source as Fig. 2-5)

SOLIDIFICACION DE METALES



Region of dendrite side arm unable to conduct away heat of freezing, and neck reheats and melts, freeing side arm



Side arm swept by convection currents into center of casting to serve as a nucleus for the formation of equiaxed grains

Fig. 2-9. Schematic illustration of the remelting of a side arm of a dendrite and movement of the side arm into the center of the casting to serve as the nucleus of an equiaxed grain.

REFUSION DE UN BRAZO DENDRITICO Y MOVIMIENTO HACIA EL CENTRO PARA LA CREACION DE UN NUCLEO EQUIAXIAL

SOLIDIFICACION DE METALES

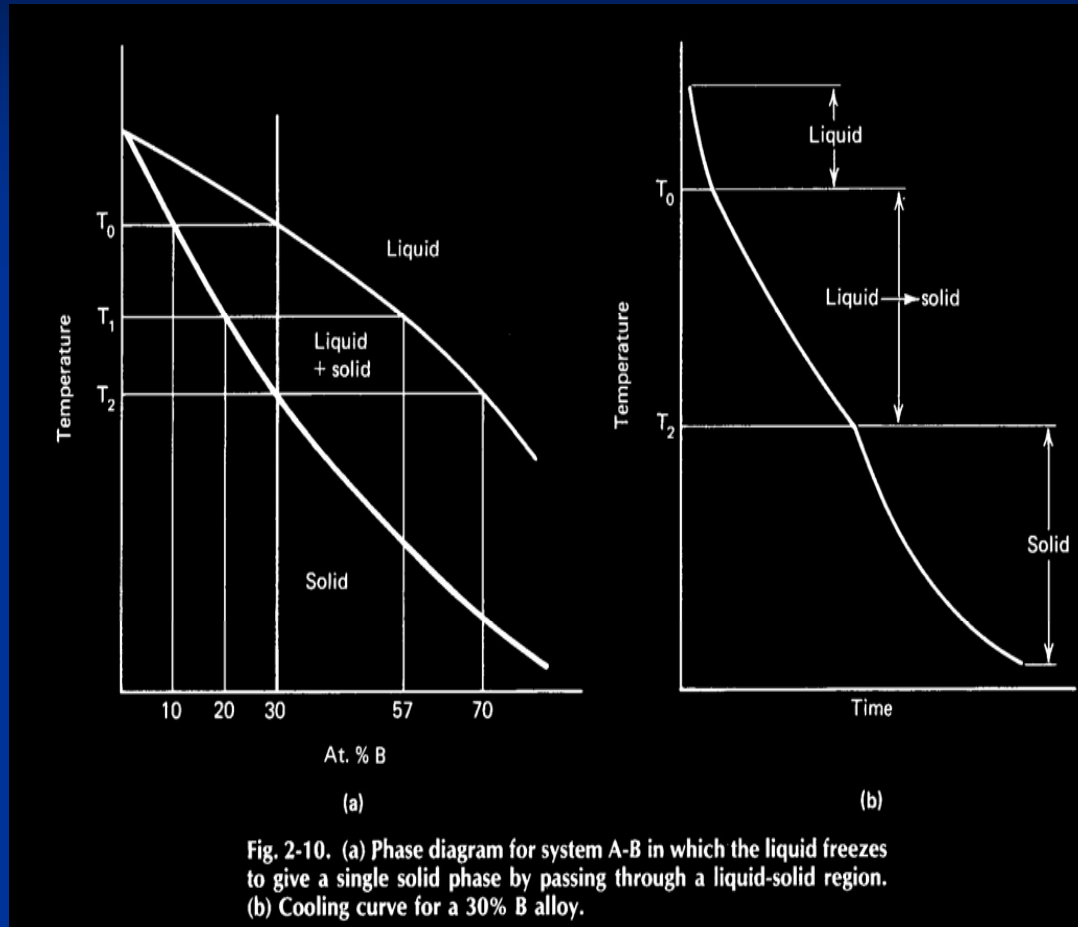


DIAGRAMA DE FASES Y CURVA DE ENFIAMIENTO PARA UNA ALEACION BINARIA DE A-B

SOLIDIFICACION DE METALES

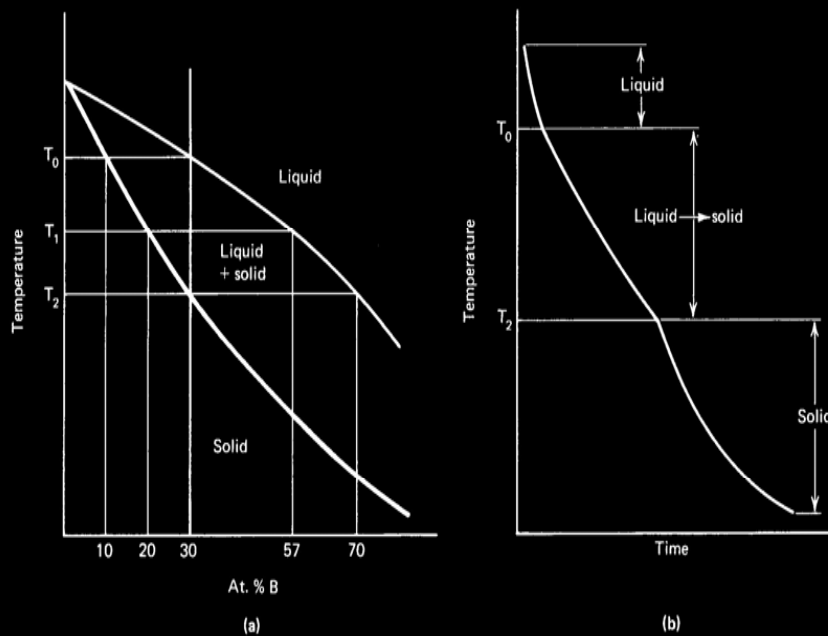


Fig. 2-10. (a) Phase diagram for system A-B in which the liquid freezes to give a single solid phase by passing through a liquid-solid region. (b) Cooling curve for a 30% B alloy.

ESQUEMA DE LAS ETAPAS DE SOLIDIFICACION DE UNA ALEACION BINARIA

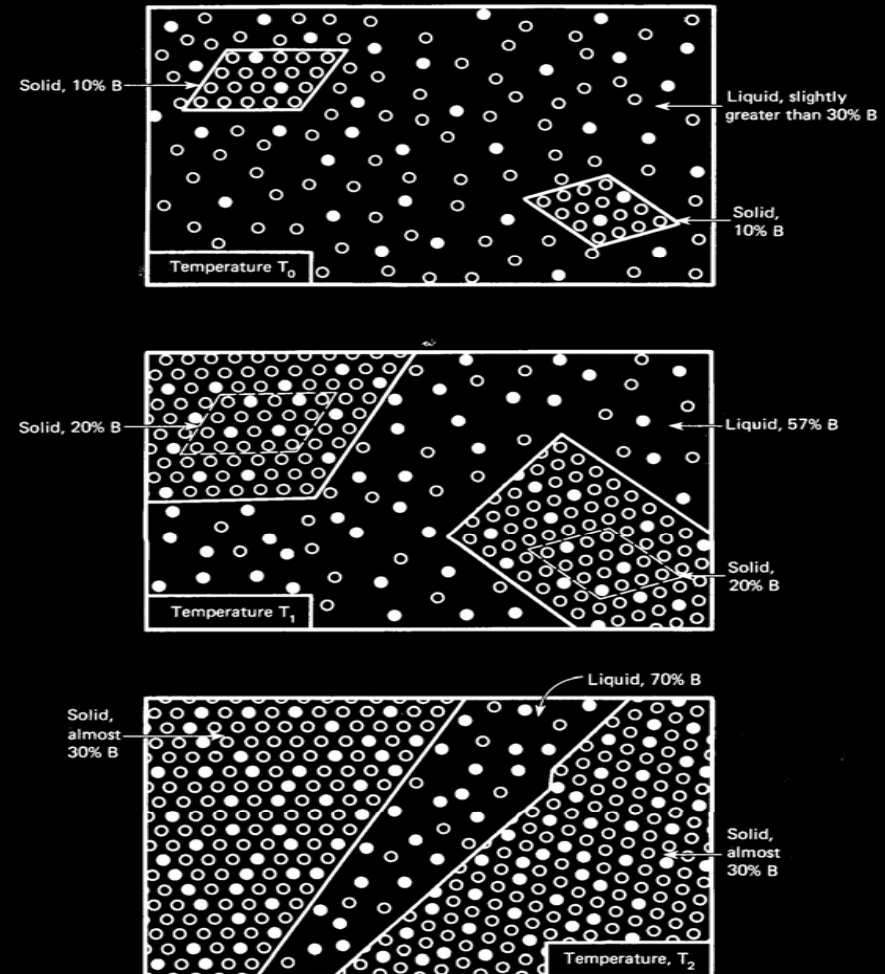
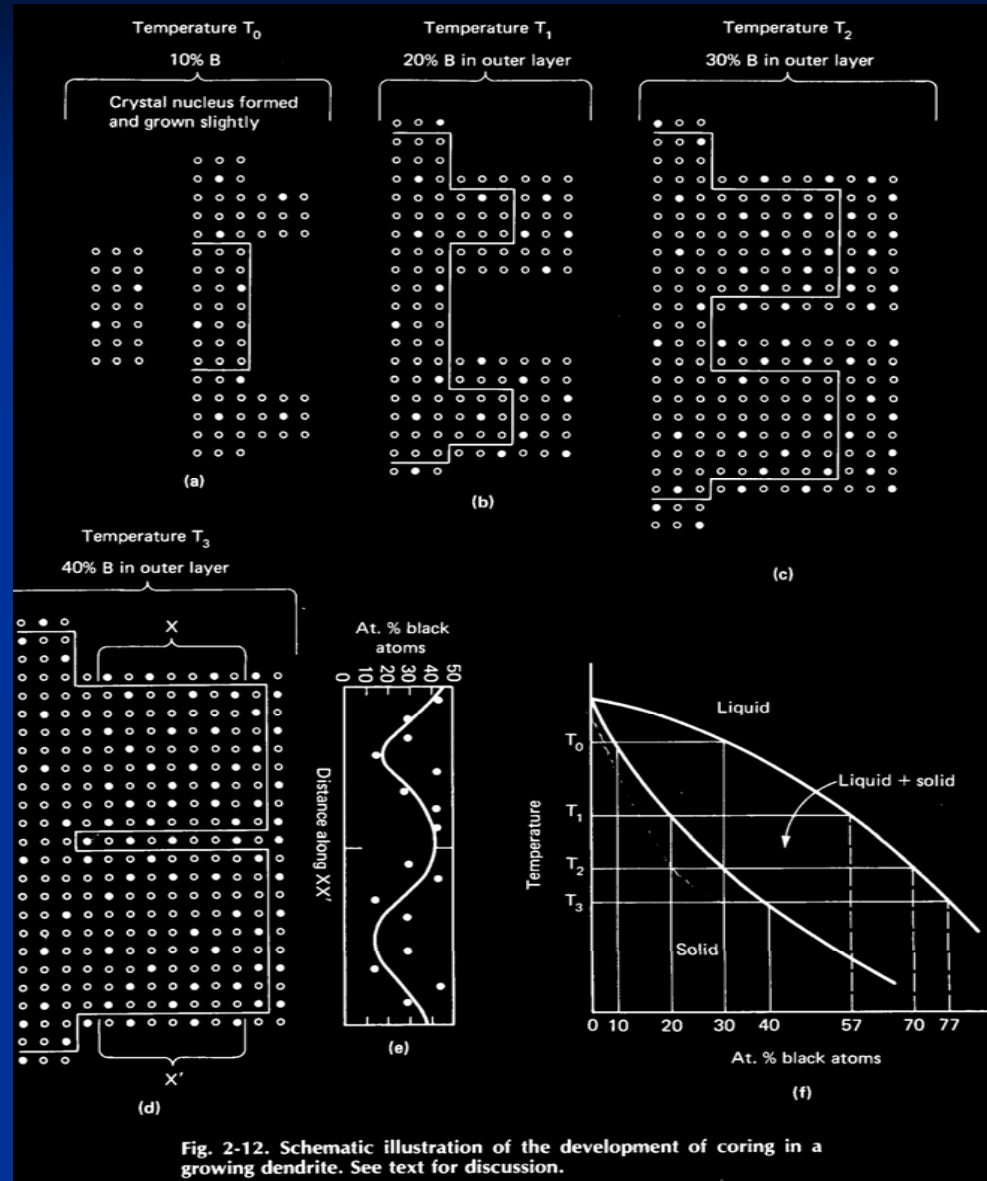


Fig. 2-11. Schematic illustration of the growth of two crystals in a 30% B alloy during equilibrium cooling. The chemical compositions of the solid and liquid are obtained from the phase diagram in Fig. 2-10(a). For simplicity, the crystals are not shown as dendrites.

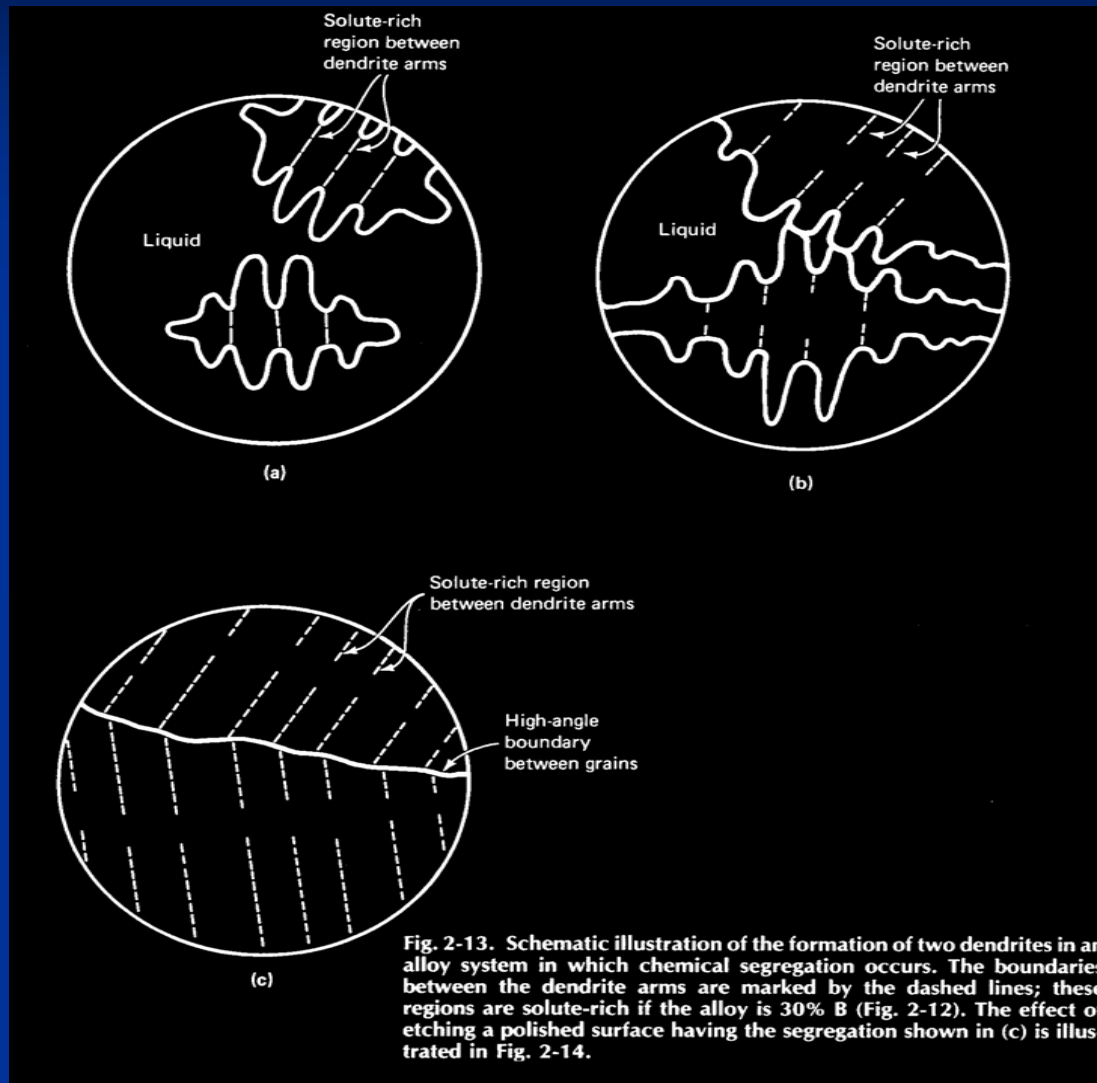
SOLIDIFICACION DE METALES

ILUSTRACION ESQUEMATICA DEL DESARROLLO DE SEGREGACION INTERDENDRITICA



SOLIDIFICACION DE METALES

FORMACION DE
DENDRITAS QUE
PRESENTAN
SEGREGACION
QUIMICA



SOLIDIFICACION DE METALES

REPRESENTACION
ESQUEMATICA DE LA
TOPOLOGIA
SUPERFICIAL PRODUCTO
DE SEGREGACION
QUIMICA DURANTE EL
CRECIMIENTO
DENDRITICO

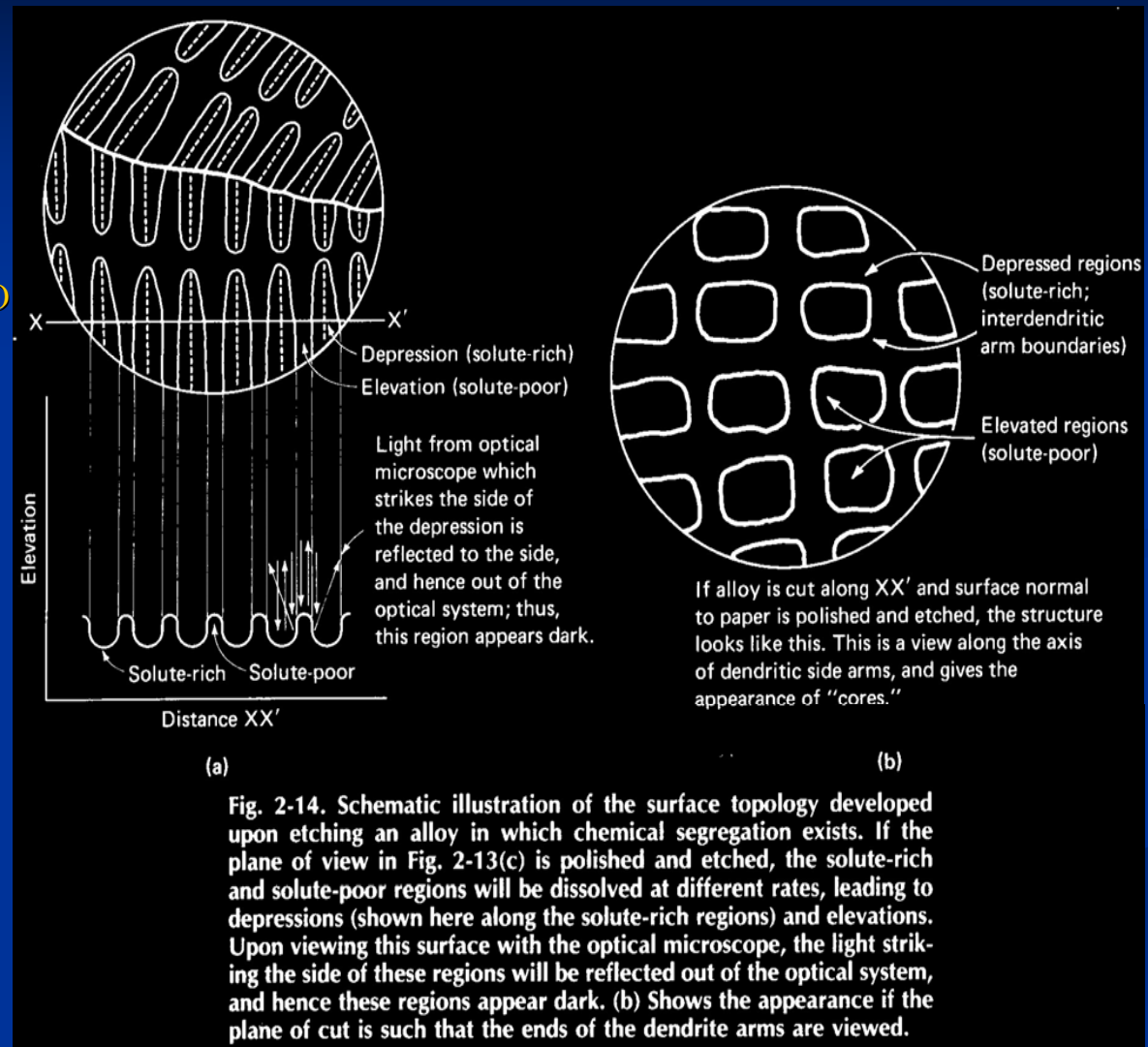
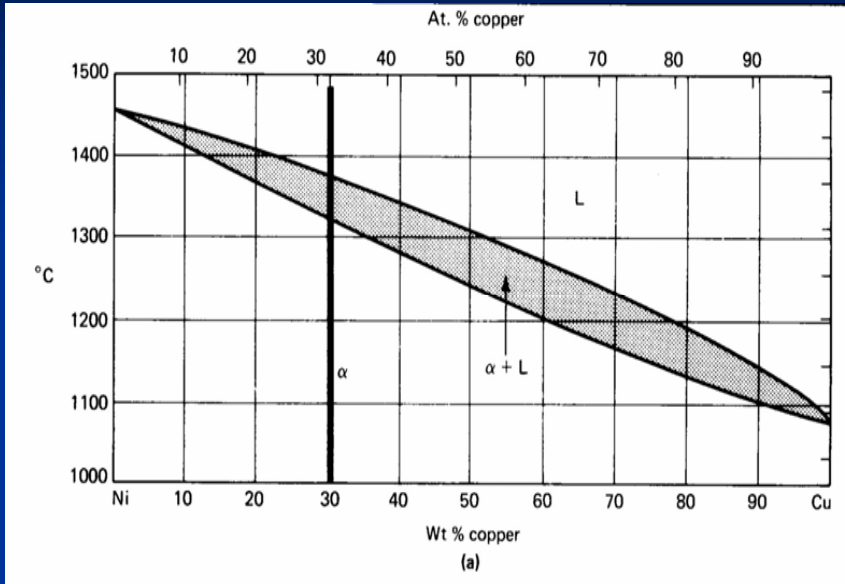


Fig. 2-14. Schematic illustration of the surface topology developed upon etching an alloy in which chemical segregation exists. If the plane of view in Fig. 2-13(c) is polished and etched, the solute-rich and solute-poor regions will be dissolved at different rates, leading to depressions (shown here along the solute-rich regions) and elevations. Upon viewing this surface with the optical microscope, the light striking the side of these regions will be reflected out of the optical system, and hence these regions appear dark. (b) Shows the appearance if the plane of cut is such that the ends of the dendrite arms are viewed.

SOLIDIFICACION DE METALES



ALEACION Ni – 30 Cu MOSTRANDO
SEGREGACION DENDRITICA

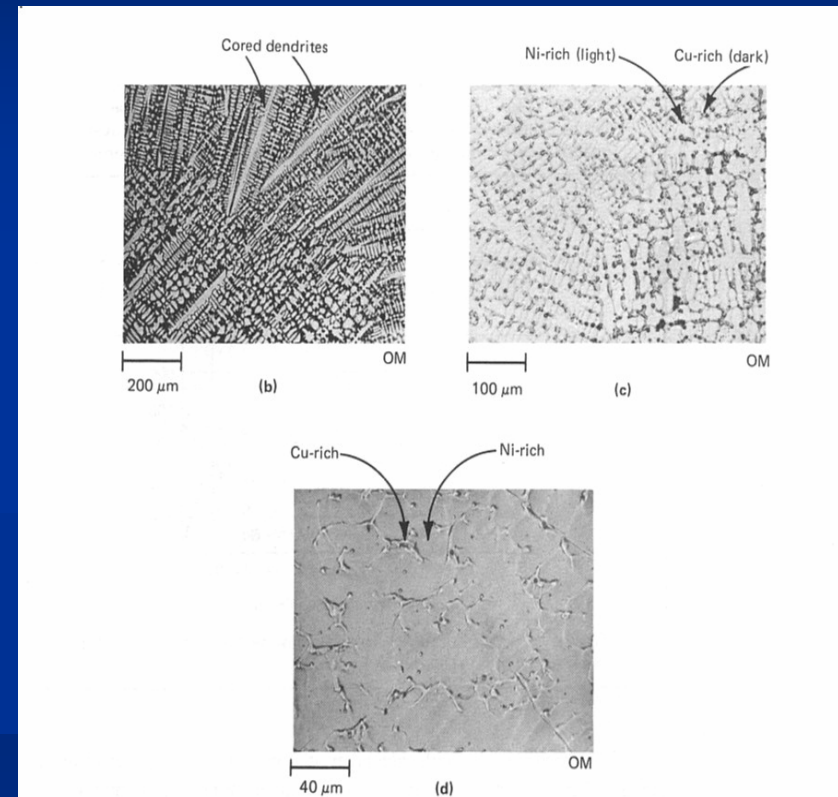
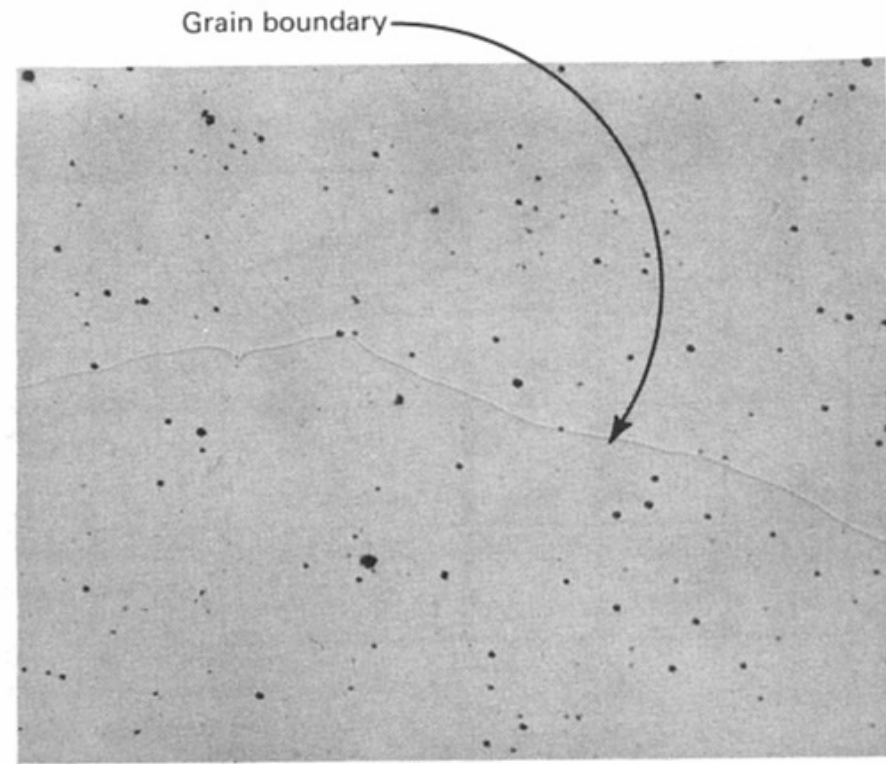


Fig. 2-15. Microstructure of a Ni-30Cu alloy which has been nonequilibrium cooled from the liquid to 20 °C. Coring is evident; this appearance originates by the mechanism described in Fig. 2-14 (especially compare with Fig. 2-14b). (Phase diagram adapted from Metals Handbook, 1948 Edition, American Society for Metals, Metals Park, Ohio)

SOLIDIFICACION DE METALES

ALEACION Ni – Cu 30
HOMOGENIZADA A
1000 °C POR 5 h Y
LUEGO ENFRIADA A
20 °C.



50 μm

OM

Fig. 2-16. Microstructure of a chill-cast Ni-30Cu alloy homogenized at 1000 °C for 5 h, then cooled to 20 °C. The microstructure before this heat treatment is shown in Fig. 2-15(b). The black dots are oxide inclusions and shrinkage cavities. Note the relative absence of coring.